Published in final edited form as:
Phys Rev Lett. 2013 January 4; 110(1): 018103.

Stress-enhanced Gelation: A Dynamic Nonlinearity of Elasticity

Norman Y. Yao[1], **Chase P. Broedersz**[2,3], **Martin Depken**[2], **Daniel J. Becker**[4], **Martin R. Pollak**[5], **Frederick C. MacKintosh**[2], and **David A. Weitz**[1]

[1]Department of Physics, Harvard University, Cambridge, MA 02138, U.S.A. [2]Department of Physics and Astronomy, VU University, Amsterdam, The Netherlands [3]Lewis-Sigler Institute for Integrative Genomics and the Department of Physics, Princeton University, Princeton, New Jersey 08544, USA [4]Renal Division, Departments of Medicine, Brigham and Women's Hospital and Harvard Medical School, Boston, Massachusetts, U.S.A. [5]Department of Internal Medicine/ Nephrology, Beth Israel Deaconess Medical Center and Harvard Medical School, Boston, Massachusetts, USA

Abstract

A hallmark of biopolymer networks is their sensitivity to stress, reflected by pronounced nonlinear elastic stiffening. Here, we demonstrate a distinct dynamical nonlinearity in biopolymer networks consisting of F-actin cross-linked by α-actinin-4. Applied stress delays the onset of relaxation and flow, markedly enhancing gelation and extending the regime of solid-like behavior to much lower frequencies. We show that this macroscopic network response can be accounted for at the single molecule level by the increased binding affinity of the cross-linker under load, characteristic of catch-bond-like behavior.

Biopolymer networks are major structural components of the cytoskleton of living cells; they exhibit a rich diversity of mechanical responses. Indeed, the complexity of cellular dynamics *in vivo* [1, 2] has prompted extensive studies of reconstituted networks *in vitro* to help elucidate nature's underlying design principles [3-5]. A ubiquitous feature of the cytoskeleton, which has been clearly elucidated through studies of reconstituted networks, is pronounced nonlinear stress-stiffening; in this case, both filaments and linkers can contribute to this static non-linearity [6-9]. Interestingly, many physiological cross-linkers are themselves transient and hence dynamical; it is this transiency which controls the structural relaxation of the network [10-13]. Typically, the interplay between stress and linker dynamics increases network fluidization, limiting solid gel-like behavior.

In this letter, we investigate a biopolymer network in which static stress does not induce yielding [14], but rather, strongly delays the onset of structural relaxation; we therefore call this behavior stress-enhanced gelation (SEG). In particular, we study the transient *physiological* cross-linker α-Actinin-4 (Actn4), a protein crucial to normal kidney function; previous studies of Actn4 have focused only on linear [11] and nonlinear elasticity [18]. By contrast, here, we show that actin-Actn4 networks exhibit a novel, dynamical form of nonlinearity distinct from the elastic stiffening observed in most biopolymer networks. To probe the molecular origin of SEG, we exploit human kidney disease-associated mutant Actn4 cross-linkers [15, 16]. Such mutations induce conformational changes of the protein, which in turn, affect its actin binding affinity; these changes in binding affinity are reflected in the network's macroscopic relaxation [17, 18]. Remarkably, applied external prestress is able to perfectly mimic the effects of mutagenesis on network dynamics. We thus propose a

PACS numbers: 87.15.La, 83.60.Df, 83.80.Rs, 87.16.Ka

molecular mechanism for stress-enhanced gelation: It results from changes in the protein conformation of the cross-linker under load, reminiscent of catch-bond-like behavior [18, 20, 21, 23].

To examine the effects of external load on transiently cross-linked networks, we measure both the linear and nonlinear mechanics of *in vitro* actin networks crosslinked with wild-type (WT) and mutant Actn4. Such networks are formed by mixing 23.8 μM (1mg/ml) G-actin solution with corresponding WT and mutant α-actinin-4 solution at a molar ratio R = 0.001 – 0.01 of Actn4 to actin. Such ratios correspond to a single-filament regime, in which the network structure is dominated by unbundled actin [19]. Full-length human recombinant Actn4 protein was expressed in and purified from baculovirus-infected Sf21 insect cells by ProteinOne (Bethesda, MD). Polymerization is initiated by the addition of 5× polymerization buffer [11] and we utilize fluorescence imaging to ensure that the resulting three-dimensional networks are free of large-scale inhomogeneities [18, 19].

The mechanical response of the network is characterized by measuring the differential storage modulus, K', and the differential loss modulus, K'' as a function of frequency [6, 25, 26]; K' represents the in-phase component of the differential shear modulus in response to a small applied oscillatory stress, while K'' represents the out-of-phase component. At frequencies above 1Hz, K' exhibits a nearly-frequency-independent plateau over which it remains significantly larger than the loss modulus; this plateau modulus determines the network stiffness as it reflects the existence of a solid-like gel, as shown by the squares in Fig. 1a. Below a clearly defined frequency, ω_R, structural relaxation sets in and both storage and loss moduli decrease dramatically: The network undergoes a transition from a clearly solid-like gel state to a power-law rheology regime where K', $K'' \sim \omega^{1/2}$ [13]. This rheology is in stark contrast to that expected for a simple Maxwell fluid [27], in spite of the single microscopic relaxation time ω_R [13]. We characterize ω_R by the local maximum in the loss modulus, as depicted in Fig. 1a [11-13].

The Actn4-F-actin network also exhibits pronounced stress-stiffening, reminiscent of other biopolymer networks [2, 4-7, 28, 29]. Upon application of an external prestress, the plateau modulus increases significantly, as shown by the circles in Fig. 1a. Moreover, the relaxation frequency also exhibits a remarkable decrease by more than an order of magnitude; interestingly, recent experiments performed on the actin-binding protein heavy meromysin (HMM) have observed analogous results [21]. Thus, the applied stress not only increases the stiffness of the network but it also dramatically extends the range (e.g. time-scale) of solid-like behavior. This is in contradistinction to the response of most materials, in which external stress typically leads to yielding and fluidization [30, 31]. The network returns to its original linear mechanical response after removal of the steady prestess, as shown by the inset of Fig. 1a. This behavior rules out shear-induced filament bundling, where one would have expected considerable differences in the network's linear rheological response following the application of an external load [32].

To characterize the gel-like behavior of the networks, we measure the inverse loss tangent (ILT), $I = K'/K''$ over a broad range of applied prestress and frequency. Larger values of ILT indicate a higher degree of network solidity and hence, a relative suppression of dissipation. With increasing prestress, the solid-like regions persist over a wider frequency range, as depicted in Fig. 1b, highlighting the stress-enhanced gelation of the network. Moreover, we find that there exist two distinct regimes of nonlinear behavior. In the first regime, at moderate values of prestress, the network exhibits only dynamic nonlinearity as evidenced by the significant shift of the relaxation frequency shown in Fig. 1c. While the range of solid-like behavior is extended in this regime, the plateau modulus remains unchanged. In the second regime, at larger values of prestress, the network exhibits stress-

stiffening, common to most biopolymer networks, as shown in Fig. 1a. At the same time, the range of solid-like behavior is even further extended.

Stress-enhanced gelation is in sharp contrast with the fluidization expected for a network under load, where an applied force can weaken the bonds between the cross-linkers and the filaments. Instead, this behavior is reminiscent of that expected for a *catch-bond*, where applied force actually strengthens rather than weakens the bond of a single molecule [20]. To explore the molecular origin of this stress-dependent bond stability and therefore of SEG itself, we exploit the existence of single point mutants of Actn4, which are known to modify the binding affinity of the linker. This allows us to explore the relationship between single-molecule binding affinity, external applied stress and network relaxation, highlighting the molecular origin of the network's macroscopic dissipation.

At the single molecule level, the actin binding domain (ABD) of α-Actinin-4 is formed from two N-terminal calponin homology (CH) domains and, like all α-Actinins, contains three actin-binding sites: ABS1-3. We utilize Actn4 linkers containing the K255E point mutation, known to cause an inherited form of human kidney disease, focal segmental glomerulosclerosis. In comparison to the WT linker, measurements of the K255E mutant exhibit a 6-fold lower equilibrium dissociation constant, implying a significantly enhanced actin binding affinity [16]. By comparison to the WT, networks formed with the K255E mutant exhibit a lower characteristic frequency for structural relaxation even in the absence of prestress, as shown in Fig. 2a. Hence, the increased bond affinity of the K255E linker leads to mutant-enhanced gelation directly analogous to the SEG seen in WT networks, clearly evincing that single molecule binding properties are reflected at the macroscopic level.

The underlying molecular origin of the K255E mutant's enhanced affinity is attributed to changes in the protein's conformation. Such conformational changes may enhance the accessibility to a latent high affinity actin binding site (ABS1) [15]. Alternatively, these conformational changes may destabilize the CH1-CH2 interface of α-Actinin-4, mitigating the steric hindrance of CH2, which otherwise weakens the linker's binding with F-actin [33].

Inspired by mutant-enhanced gelation, we also demonstrate enhanced network fluidization; we do so, by exploiting the QTAA mutant Actn4, a cross-linker known to exhibit a lower actin binding affinity. Networks formed with the QTAA mutant do indeed exhibit a higher characteristic frequency for structural relaxation, leading to a more fluid-like structure over the full range of frequencies probed, as depicted in Fig. 2a.

To further explore the role of binding affinity, we use the double mutant (DM) K255E/QTAA, whose two point mutations have opposite effects; therefore, in the absence of prestress, the DM binding affinity should revert back to a value approximately equal to that of WT Actn4 [18]. This is in fact confirmed by the data: Networks formed with the DM mutant exhibit a characteristic frequency for structural relaxation nearly identical to that of WT networks, as illustrated in Fig. 2a. This provides further support for the crucial role that affinity plays in the enhanced stability of the Actin-K255E bond [16].

The similarity of the functional form for all of the data with mutant cross-links to that of the data with WT cross-links, both with and without prestress, suggests that the full mechanical response of all networks can be characterized within the framework of linker dynamics and entropic stiffening [13]; this is indeed highlighted by the scaling of *all* data onto the same universal curve, as shown in Fig. 2b. Moreover, this similarity also evinces a possible molecular origin for the observed catch-bond-like behavior of the WT linker: It results from a *load-induced* protein conformational change, leading to a relaxation rate similar to that of the K255E mutant. Interestingly, this demonstrates that external prestress may be able to

control the relative exposure of ABS1 or the relative stability of the CH1-CH2 interface [16, 33].

Our proposed molecular catch-bond picture is consistent with all of the observed macroscopic rheology. Further evidence is found at the highest applied stresses before network rupture, where the WT relaxation rate approaches the zero stress K255E relaxation rate $\omega_R \approx 0.03$ Hz, as shown in Fig. 2c. Moreover, for the full range of molar ratios probed ($R = 0.001 – 0.01$), the network dynamics (e.g. relaxation frequency dependence and onset frequency) are consistent [13, 18]. Nonetheless, an alternative explanation for this catch-bond behavior can arise from a collective, network-level, geometric effect [21, 22]. While such geometry may play a role in the network's enhanced gelation [21, 22], it would not, however, explain the observed changes in the microscopic dissociation constant, K_d, of mutant forms of Actn4 [16]. Indeed, the fact that our observed shifts in macroscopic relaxation timescales are mirrored in microscopic changes of K_d suggests that the observed catch-bond-like behavior may be dominated by Actn4's underlying molecular structure. Although K_d characterizes only the ratio of the linker's off- to on-rate, since k_{on} is typically diffusion-limited, changes in K_d directly reflect changes in the linker's binding affinity, and hence, the network's relaxation time. We emphasize that additional single molecule experiments are important to fully elucidate the nature of Actn4 and to clarify the interplay between geometry and molecular structure.

If stress-enhanced gelation arises from load-induced changes to the WT-protein conformation, these effects should be abrogated in networks formed with the K255E mutant, which already harbors an exposed ABS1 site. Thus, we probe the rheological response of K255E crosslinked networks under varying amounts of external prestress. The ILT contours of the K255E mutant are nearly horizontal and do not significantly expand in frequency range as the prestress increases, as shown in Fig. 1d. This reflects a sharply suppressed SEG response by comparison to the WT contours, which exhibit significantly enlarged regions of solid-like behavior as the prestress increases. Here, the distinction between SEG and simple nonlinear stiffening is especially apparent: Despite a suppressed SEG response, the elastic modulus of the K255E mutant networks nevertheless increases with stress [18]. At the highest stresses achieved before network rupture, the frequency range of solid-like behavior is sharply reduced, indicating enhanced fluidization. This impending fluidization may reflect the inevitable onset of Bell-like behavior due to the load-induced rupturing of the linker-filament bond [35]. This transition to Bell-like behavior is not directly seen in the WT ILT contours. Nevertheless, the WT contours do flatten at the highest prestresses, analogous to the suppressed SEG of the K255E mutant, strongly suggesting incipient Bell-like behavior.

The stress-dependent viscoelastic behavior of Actn4-F-actin networks exhibits three distinct regimes: At the lowest applied stresses ($\sigma < 1.5$Pa), the network behavior is fully linear, with both K' and ω_R independent of prestress. As stress increases, ($1.5\text{Pa} < \sigma < 4\text{Pa}$), the elastic modulus remains unchanged, whereas the region of gelation is expanded, as the relaxation frequency decreases from $\omega_R = 0.5$Hz to $\omega_R = 0.1$Hz. At the highest stresses ($\sigma >$ 4Pa) the elastic plateau modulus also exhibits nonlinear behavior, consistent with $K' \sim \sigma^{3/2}$, as predicted by theory for the entropic stretching of semiflexible filaments [6, 29]. These results are summarized by plots of the stress-dependence of both K' and ω_R in Fig. 2c.; these data highlight the existence of three distinct rheological behaviors: linear, dynamically nonlinear, and elastically nonlinear.

The origin of these three distinct regimes can be understood physically through a combination of the molecular behavior of the cross-linker and the rheology of the network. In the limit of low external prestress, neither the linker's actin binding affinity, nor the filament's thermal fluctuations are dramatically affected; this limit corresponds to the

maximal linker unbinding rate. Physically, this may correspond to a hidden ABS1 site, as shown schematically in Fig. 2d. As the applied stress is increased, the Actn4 conformation begins to open, exposing the previously hidden ABS1 site and thereby increasing the linker's actin affinity. This leads to a corresponding decrease in the linker's unbinding rate, resulting in dynamic nonlinearity. However, at such moderate stresses, the thermal fluctuations governing the network's plateau modulus are unaffected, and hence the elasticity remains linear. By contrast, at the highest stresses, the thermal fluctuations of the actin filaments are pulled out leading to entropically driven stress-stiffening and thus elastic nonlinearity, as depicted in Fig. 2d. The independence of linker conformation and network entropy can thus naturally explain the appearance of two distinct nonlinear regimes.

Stress-enhanced gelation could have important biological consequences relating to the mechanisms of intracellular remodeling and dynamic stress accommodation. Combined with myosin activity, SEG would enable the actin cytoskeleton to independently control both the network stiffness and the frequency range of solid-like behavior. Prior work has shown that contractile myosin activity can lead to stiffening of model actin networks [36]. The present results suggest that such activity can also modulate the onset of fluidization. Thus, by varying myosin motor activity, the cell can actively tune the internal tension of its cytoskeleton, thereby accessing a full range of network mechanics and relaxation. This is qualitatively demonstrated by experiments on airway smooth muscle cells where myosin driven contractile stresses control the transition between fluid- and solid-like behavior [37]. Remarkably, the cellular solidity, as measured by the inverse loss tangent, increases as a function of increasing contractile stress, suggesting that SEG does in fact manifest *in vivo* [38]. This attests to the importance of understanding the stress-dependent mechanics of reconstituted biopolymer networks. Further study is required to fully elucidate the SEG behavior in such cells; particularly intriguing is the possible interplay between myosin-driven enhanced gelation and actin bundles that organize as stress fibers. Finally, complementary studies at the single molecule level could provide additional insights into the underlying molecular mechanism.

Acknowledgments

We gratefully acknowledge the insights of and conversations with Sirfyl and Jubowers. This work was supported in part by the National Science Foundation (DMR-1006546), the Harvard Materials Research Science and Engineering Center (DMR-0820484), the United States Department of Energy (FG02-97ER25308), the NIH (DK59588 and DK083592) and the Foundation for Fundamental Research on Matter and the Netherlands Organization for Scientific Research.

References

[1]. Bray D, White JG. Science. 1988; 239:883. [PubMed: 3277283]

[2]. Fletcher DA, Mullins RD. Nature (London). 2010; 463:485. [PubMed: 20110992]

[3]. Janmey PA, Hvidt S, Lamb J, Stossel TP. Nature (London). 1990; 345:89. [PubMed: 2158633]

[4]. Bausch AR, Kroy K. Nature Physics. 2006; 2:231.

[5]. Kasza KE, et al. Current Opinions in Cell Biology. 2007; 19:101.

[6]. Gardel ML, et al. Science. 2004; 304:1301. [PubMed: 15166374]

[7]. Storm C, Pastore JJ, MacKintosh FC, Lubensky TC, Janmey PA. Nature. 2005; 435:191. [PubMed: 15889088]

[8]. Wagner B, Tharmann R, Haase I, Fischer M, Bausch AR. Proc. Natl. Acad. Sci. USA. 2006; 103:13974. [PubMed: 16963567]

[9]. Kasza KE, et al. Phys. Rev. E. 2009; 79:041928.

[10]. Wachsstock DH, Schwartz WH, Pollard TD. Biophys. J. 1993; 65:205. [PubMed: 8369430]

[11]. Volkmer-Ward SM, Weins A, Pollak MR, Weitz DA. Biophys. J. 2008; 95:4915. [PubMed: 18689451]

[12]. Lieleg O, Claessens MMAE, Luan Y, Bausch AR. Phys. Rev. Lett. 2008; 101:108101. [PubMed: 18851260]

[13]. Broedersz CP, Depken M, Yao NY, Pollak MR, Weitz DA, MacKintosh FC. Phys. Rev. Lett. 2010; 105:238101. [PubMed: 21231506]

[14]. Sprakel J, Lindstrom SB, Kodger TE, Weitz DA. Phys. Rev. Lett. 2011; 106:248303. [PubMed: 21770607]

[15]. Weins A, et al. Journal of the American Society of Nephrology. 2005; 16:3694. [PubMed: 16251236]

[16]. Weins A, et al. Proc. Natl. Acad. Sci. USA. 2007; 104:16080. [PubMed: 17901210]

[17]. Wachsstock DH, et al. Biophys. J. 1994; 66:801. [PubMed: 8011912]

[18]. Yao NY, et al. J. Mol. Biol. 2011; 411:1062. [PubMed: 21762701]

[19]. Lieleg O, Schmoller KM, Cyron CJ, Luan Y, Wall WA, Bausch AR. Soft Matter. 2009; 5:1796.

[20]. Thomas WE, Vogel V, Sokurenko E. Annual Review of Biophysics. 2008; 37:399.

[21]. Lieleg O, Schmoller KM, Claessens MMAE, Bausch AR. Biophys. J. 2009; 96:4725. [PubMed: 19486695]

[22]. Suzuki Y, Dudko OK. Phys. Rev. Lett. 2010; 104:048101. [PubMed: 20366741]

[23]. Norstrom M, Gardel ML. Soft Matter. 2011; 7:3228. [PubMed: 21552431]

[24]. Lieleg O, Claessesens MMAE, Bausch AR. Soft Matter. 2010; 6:218–225.

[25]. Yao NY, Larsen RJ, Weitz DA. J. Rheology. 2008; 52:1013.

[26]. Broedersz CP, et al. Soft Matter. 2010; 6:4120.

[27]. Larson, RG. The Structure and Rheology of Complex Fluids. Oxford University Press; Oxford: 1995.

[28]. Lin Y-C, et al. Phys. Rev. Lett. 2010; 104:058101. [PubMed: 20366795]

[29]. MacKintosh FC, Kas J, Janmey PA. Phys. Rev. Lett. 1995; 75:4425. [PubMed: 10059905]

[30]. Mason TG, Weitz DA. Phys. Rev. Lett. 1995; 75:2770. [PubMed: 10059400]

[31]. Sollich P, Lequeux F, Hebraud P, Cates ME. Phys. Rev. Lett. 1997; 78:2020.

[32]. Schmoller KM, et al. Nat. Comm. 2010; 1:134.

[33]. Galkin VE, et al. Nature Struct. Mol. Biol. 2010; 17:614. [PubMed: 20383143]

[34]. Gittes F, MacKintosh FC. Phys. Rev. E. 1998; 58:R1241.

[35]. Bell GI. Science. 1978; 200:618. [PubMed: 347575]

[36]. Mizuno D, Tardin C, Schmidt CF, MacKintosh F. Science. 2007; 315:370. [PubMed: 17234946]

[37]. Stamenovic D, Suki B, Fabry B, Wang N, Fredberg JJ, Buy JE. J. Appl. Physiol. 2004; 96:1600. [PubMed: 14707148]

[38]. Kollmannsberger P, Fabry B. Annu. Rev. Mater. Res. 2011; 41:75.

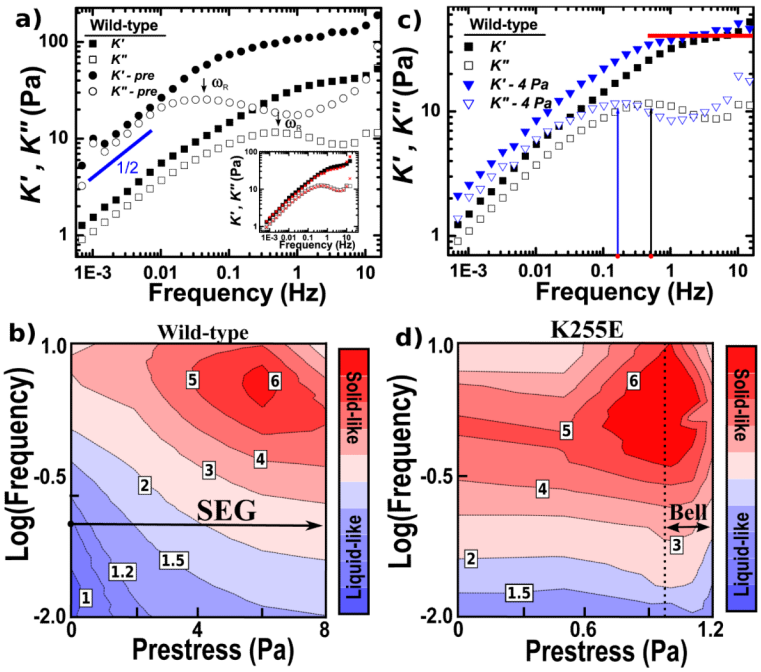

FIG. 1.

(color online) a) Depicts frequency sweeps of the differential storage (K') and loss (K'') moduli of WT cross-linked networks under zero prestress (squares) [13] and under significant prestress (circles). The prestress data is acquired just before network rupture at ~ 9Pa. (Inset) Demonstrates the recovery of the linear mechanical response (red crosses) following measurements of nonlinear elasticity at 8.7Pa [18]. b) Depicts a contour plot of the WT ILT= K'/K'' as a function of both frequency and prestress. Individual data points are located in frequency at: 17 log-spaced points between 6.94×10^{-4} Hz and 15 Hz, and in prestress at: 0, 2, 4, 6, 8Pa. We utilize a third-order spline interpolation to fit the data to generate smooth contours. c) At intermediate levels of prestress, the plateau modulus remains unchanged (red line). However, the relaxation frequency ω_R (arrows) has already decreased, demonstrating a clear separation between network stiffening and the dynamic nonlinearity which underlies SEG. d) Depicts a contour plot of the K255E ILT= K'/K'' as a function of both frequency and prestress. Individual data points are located at the same frequencies as b) and in prestress at: 0, 0.5, 1, 1.1, 1.2Pa. All of the above data is taken at R = 0.01.

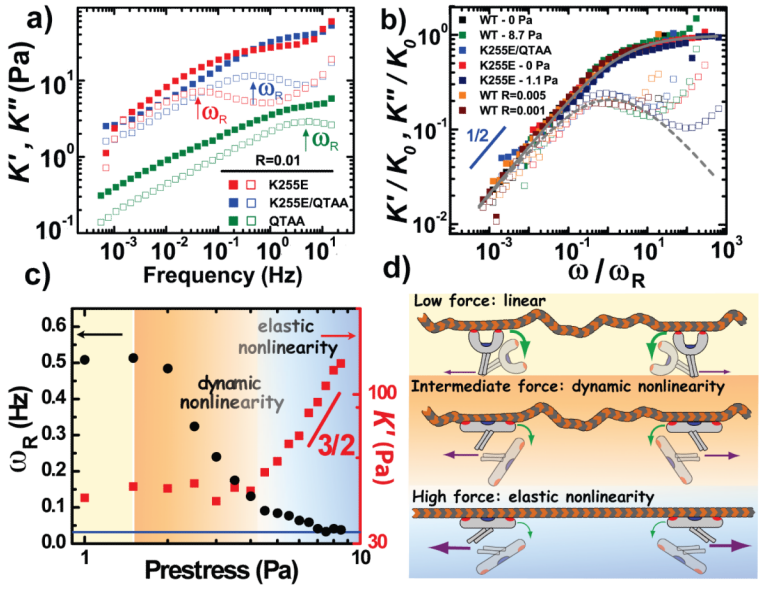

FIG. 2.

(color online) a) Depicts frequency sweeps of the viscoelastic moduli for K255E, QTAA and double-mutant Actn4 cross-linked networks without external prestress (data from [18]). (b) Shows the clear collapse of the viscoelastic response for a wide variety of network compositions onto the universal theory curve. The theoretical predictions for the elastic (solid) and viscous (dashed) response are obtained from the mean-field CGD model of [13] with $t_{eq} \rightarrow 0$. It is important to note that the collapse is expected to fail at the highest frequencies, as born out by the data, both due to instrument inertial effects and viscous dynamics [34]. c) Depicts the three distinct regimes of WT network behavior, characterized as linear (yellow), elastically nonlinear (blue), and dynamically nonlinear (orange). The relaxation frequency ultimately approaches the zero stress K255E relaxation rate $\omega_R \approx 0.03$ Hz (represented by the blue line). d) Schematic illustration of the molecular origin of the three regimes of mechanical response [18]. At the lowest levels of prestress (purple arrow), the system is linear and the filaments exhibit thermal fluctuations as evidenced by the contortions of the polymer. In this regime, the linker's unbinding rate (green arrow), which corresponds to ω_R, is also maximal. As the prestress increases, the conformational state of the linker changes and the ABS1 site is exposed. This induces a catch-bond-like behavior where cross-linking is stabilized by force, slowing down the relaxation dynamics and significantly decreasing ω_R. However, the applied stress is not yet strong enough to have pulled out the fluctuations of the filament; thus, the network stiffness remains unchanged. Finally, at the highest prestresses, the fluctuations of the filament are pulled out and the network depicts entropic stress-stiffening with a dramatic increase in the network's plateau modulus.